Studies in Fungi

ARTICLE

Open Access

https://doi.org/10.48130/sif-0025-0010
Studies in Fungi **2025**, 10: e010

New records of *Neopestalotiopsis* species associated with leaves of *Annona muricata* (Soursop) and *Garcinia mangostana* (Mangosteen) in the Western Province, Sri Lanka, and *in vitro* evaluation of selected biocontrol agents for their growth suppression

Fathima Asfa[1], Kasun M. Thambugala[1,2,3*], Dinushani A. Daranagama[4], Nimali I. de Silva[5], Kapila K Liyanage[6] and Samawansha H. Tennakoon[1]

[1] *Genetics and Molecular Biology Unit, Faculty of Applied Sciences, University of Sri Jayewardenepura, Gangodawila, Nugegoda 10250, Sri Lanka*
[2] *Center for Plant Materials and Herbal Products Research, University of Sri Jayewardenepura, Nugegoda 10250, Sri Lanka*
[3] *Center for Biotechnology, Department of Zoology, University of Sri Jayewardenepura, Nugegoda, Sri Lanka*
[4] *Department of Plant and Molecular Biology, Faculty of Science, University of Kelaniya, Kelaniya 11300, Sri Lanka*
[5] *Shenzhen Key Laboratory of Microbial Genetic Engineering, College of Life Sciences and Oceanography, Shenzhen University, Shenzhen 518060, P.R. China*
[6] *Rubber Research Institute of Sri Lanka, Dartonfield, Agalawatta, Sri Lanka*
* Corresponding author, E-mail: kasun@sci.sjp.ac.lk

Abstract

Most pestalotioid species are phytopathogens characterized by conidia with appendages and can also function as endophytes and saprobes. During a morpho-molecular study of plant-inhabiting micro-fungi in Sri Lanka, two pestalotioid species were isolated from the lesions of living leaves of *Garcinia mangostana* and *Annona muricata*. Maximum Likelihood and Bayesian Inference analyses of combined internal transcribed spacers (ITS), β-tubulin (*tub2*), and translation elongation factor 1-α (*tef1-*α) sequence data were used to determine the phylogenetic affinities of the collected species. Detailed morphological and multi-locus phylogenetic analyses further validated that the collected pestalotioid species belonged to *Neopestalotiopsis*. *Neopestalotiopsis cubana* (GMBUCC 24–001) and *N. scalabiensis* (GMBUCC 24–002 and GMBUCC 24–003) were identified as associated with the fresh leaves of *G. mangostana* and *A. muricata,* respectively. This is the first record of the *Neopestalotiopsis* species associated with these hosts worldwide. This study evaluated the *in vitro* biocontrol potential of *Trichoderma atroviride* (GMBUCC 24–014) and *Daldinia eschscholtzii* (UKBC 036) against *Neopestalotiopsis cubana* and *N. scalabiensis*, resulting in significant biocontrol potential of *T. atroviride* (GMBUCC 24–014) against both species than *D. eschscholtzii* (UKBC 036). Accurate identification of pestalotioid species is crucial for developing effective biocontrol methods to manage diseases and enhance economic development.

Citation: Asfa F, Thambugala KM, Daranagama DA, de Silva NI, Liyanage KK, et al. 2025. New records of *Neopestalotiopsis* species associated with leaves of *Annona muricata* (Soursop) and *Garcinia mangostana* (Mangosteen) in the Western Province, Sri Lanka, and *in vitro* evaluation of selected biocontrol agents for their growth suppression. *Studies in Fungi* 10: e010 https://doi.org/10.48130/sif-0025-0010

Introduction

Pestalotioid species are a group of fungi that cause a variety of diseases in a range of different hosts worldwide. Most pestalotioid species have their asexual morph with appendages bearing conidia and are extensively dispersed in tropical and temperate regions. It is well known that most of the identified pestalotioid species are phytopathogens[1,2]. In contrast, some are endophytes that can produce several bioactive compounds with potential applications in medicine, agriculture, and various industries[1–3]. Due to their ability to switch nutritional modes, many phytopathogenic and endophytic pestalotioid species occur as saprobes inhabiting dead leaves, bark, and twigs[1,4–7]. Fungal taxonomists have increasingly relied on multi-locus phylogeny combined with morphological characteristics for species identification. Pestalotioid taxa were segregated into three genera: *Pestalotiopsis, Neopestalotiopsis,* and *Pseudopestalotiopsis* in the family Sporocadaceae, which was introduced by Corda in 1842[8,9]. The conidial morphology of *Pestalotiopsis, Neopestalotiopsis,* and *Pseudopestalotiopsis* is largely identical, comprising five cells: a basal cell with a single appendage, a hyaline apical cell with one or more appendages, and three pigmented median cells. However, the color of the pigmented cells differentiates these taxa, with *Pseudopestalotiopsis* and *Pestalotiopsis* being concolorous, while *Neopestalotiopsis* exhibits versicolorous pigmentation. Although *Pestalotiopsis* and *Pseudopestalotiopsis* share similar conidial morphologies, they can be distinguished by having three slightly darker pigmented cells in *Pseudopestalotiopsis*[1,4–6]. Sexual morphs are rare among *Pestalotiopsis*[1], *Pseudopestalotiopsis*[6] , and *Neopestalotiopsis*[1,3] species. Distinguishing between the sexual morphs of *Pseudopestalotiopsis* based solely on morphology is challenging due to their close resemblance to *Pestalotiopsis*[1,6,7]. Therefore, researchers have increasingly relied on multigene phylogeny combined with morphological characteristics to identify the *Pestalotiopsis* and allied genera[1,6,10,11].

Members of *Neopestalotiopsis* are commonly distributed in tropical and subtropical ecosystems worldwide as phytopathogens, endophytes, or saprobes[1,3]. Furthermore, common phytopathogens of *Neopestalotiopsis* are associated with a variety of plant diseases, including shoot and twig dieback[12,13], leaf spots[14–16], crown rot[17], leaf blight[17–19], fruit rot[20,21], flower drying[22,23], and leaf fall diseases[24–26]. They also contribute to postharvest diseases in fruits such as mango, rose apple, mangosteen, strawberry, and

avocado[20,27,28]. Over the past few years, a significant number of *Neopestalotiopsis* species have been described, highlighting the remarkable species diversity within this genus. The genus currently comprises 127 taxa (Mycobank 2025: www.mycobank.org/page/Home). Further investigations of pestalotioid fungi are likely to uncover additional *Neopestalotiopsis* species and provide insights into their ecological interactions.

Garcinia mangostana (mangosteen) and *A. muricata* (soursop) are tropical fruit trees, distributed mainly in tropical and subtropical countries, including Sri Lanka. Economically important plants such as *G. mangostana* (mangosteen) and *A. muricata* (soursop), cultivated in Sri Lanka, are also susceptible to pestalotioid phytopathogens. Unraveling the molecular phylogeny of pestalotioid species causing leaf lesions in *G. mangostana* and *A. muricata* in Sri Lanka has practical implications for disease management, agriculture, biodiversity, and economic conservation. Molecular diagnostic tools can be used for the early detection of plant diseases and timely intervention, helping to mitigate the economic losses associated with pathogen-associated infections. Furthermore, accurate identification of the pathogens using detailed molecular and morphological identification is essential for developing effective biocontrol methods to manage the diseases they cause, thereby supporting economic development. Most pestalotioid taxa in Sri Lanka are recognized as phytopathogens with no host specificity. Therefore, this study aims to identify pestalotioid species associated with the leaves of *G. mangostana* and *A. muricata* in Sri Lanka based on comprehensive molecular phylogenetic analyses and morphological characterization to establish the taxonomic placement of the identified pestalotioid species. Furthermore, the present study evaluates the biocontrol potential of *T. atroviride* and *Daldinia eschscholtzii* against the isolated pestalotioid species using dual culture plate assays.

Materials and methods

Sample collection, isolation, and morphological identification

Symptomatic fresh leaves of *G. mangostana* (mangosteen) and *A. muricata* (soursop) were collected from Kadawatha, Gampaha District, Sri Lanka, and transferred to the laboratory using labelled zip-lock plastic bags. The micro-morphological characters of the specimens, such as conidial length, width, length, colour of median cells, and number of apical appendages, were examined and photographed using an Optika Trinocular Phase Contrast Microscope (B-510ASB, Italy) with a digital camera. All microscopic measurements were made with the Tarosoft image framework (v. 0.9.0.7).

Single spore isolation was carried out following the method described by Senanayake et al.[14]. Germinated conidia were aseptically transferred into fresh PDA plates and incubated at 28 °C to obtain pure cultures. Cultures were incubated at room temperature (28 °C) for 7–14 d. Cultures were later transferred to PDA slants and stored at 4 °C for further studies. Generated cultures were deposited at the culture collection of the Genetics and Molecular Biology Unit, University of Sri Jayewardenepura, Sri Lanka. Colony characteristics were recorded from cultures grown on potato dextrose agar (PDA). Herbarium specimens were deposited in the herbarium of the Department of Botany (USJ-H) and the Genetics and Molecular Biology Unit (USJ-GMBU) of the Sri Jayewardenepura University of Sri Lanka. Fungal isolates were deposited in the Culture Collection of the Genetics and Molecular Biology Unit (GBMUCC), University of Sri Jayewardenepura, Sri Lanka.

DNA extraction, PCR amplification, and agarose gel electrophoresis

Approximately 75–100 mg of the scraped axenic mycelia was transferred into labeled 1.5 mL microfuge tubes. Genomic DNA was extracted from the mycelia using the CTAB method, following the protocol described by Thambugala et al.[29]. Three loci (ITS, *tub2* and *tef1*) were amplified, *β*-tubulin (*tub2*) with primers Bt2a/Bt2b[30]; internal transcribed spacer region of ribosomal DNA (ITS: ITS5/ITS4)[31] and the translation elongation factor 1-alpha gene (*tef1*: EF1-526F/EF1-1567R)[32]. The amplification reactions were performed in 25 µl volumes containing 8.5 µl of sterilized H2O, 10.5 µl of Go Taq® Hot Start Green Master Mix (mixture of Go Taq Hot Start Polymerase, dNTPs, and optimized buffer (Promega)), 2 µl of 25 mM $MgCl_2$, 1 µl of each forward and reverse primer, and 2 µl of DNA template (1.2 µg/ml). The PCR thermal cycle program for ITS amplification was provided initially at 94 °C for 3 min, followed by 35 cycles of denaturation at 94 °C for 1 min, annealing at 55 °C for 1 min, elongation at 72 °C for 1 min, and final extension at 72 °C for 10 min. The PCR thermal cycle program for *tub2* and *tef1* gene amplification was provided with the same, except for the annealing temperature, which was used as 57.5 °C and 56 °C, respectively. The PCR results were observed on 1.2% agarose electrophoresis gels stained with ethidium bromide under ultraviolet light. Subsequently, PCR product purification and Sanger sequencing were performed at Genelabs Medical (Pvt) Ltd, Sri Lanka.

Sequencing and phylogenetic analyses

For the newly synthesized sequences in this study, a consensus sequence was derived using DNASTAR Lasergene SeqMan Pro v.8.1.3 from the sequences obtained from both forward and reverse primers. Low-quality end fragments of the DNA sequences were removed using the BioEdit program. A total of 120 strains belonging to the *Neopestalotiopsis* were included to construct the updated phylogenetic tree. The outgroup taxon used was *Pestalotiopsis trachycarpicola* (OP068).

The DNA sequences were subjected to BLASTn searches, and the reference nucleotide sequences for the phylogenetic analyses were retrieved from GenBank based on published data. Separate single-gene alignments for ITS, *tub2,* and *tef1* were performed using MUSCLE in MEGA11. The alignments were visually inspected and manually corrected when necessary. Single-gene phylogenies were inferred for ITS, *tub2,* and *tef1*, followed by a combined multigene analysis to more accurately resolve closely related species. GenBank numbers and culture collection (strains) numbers of the taxa included in the phylogenetic analyses are in Table 1.

The phylogenetic analysis was conducted using the maximum likelihood (ML) method, employing RAxML-HPC BlackBox (8.2.4) on the CIPRES portal. The GTR + I + G model of evolution was applied in this analysis[35,36]. Bayesian Inference (BI) was performed using MrBayes v. 3.1.2[37] to evaluate posterior probabilities (PP) by Markov Chain Monte Carlo sampling (MCMC)[38,39]. The posterior probability distribution convergence was ensured by running 1,000,000 generations of Markov chain Monte Carlo (MCMC) with a random seed and a stop value = 0.01, using a MCMC algorithm of four chains. The initial 20% of the sampled data were discarded as burn-in. Phylograms were visualized with FigTree v1.4.0[40] and annotated in Microsoft PowerPoint (2010).

In vitro antifungal activity of *Trichoderma atroviride* (GMBUCC 24–014) and *Daldinia eschscholtzii* (UKBC 036) against pestalotioid species using dual culture plate assay

Bio–control potential of *Trichoderma atroviride* (GMBUCC 24–014, Konara et al.[51]) and *Daldinia eschscholtzii* (UKBC 036, Thambugala

Table 1. Details of the *Neopestalotiopsis* strains included in this study.

Species	Culture collection number	ITS	*tub2*	*tef1*	Ref.
Neopestalotiopsis acrostichi	MFLUCC 17–1754^T	MK764272	MK764338	MK764316	[53]
N. acrostichi	MFLUCC 17–1755	MK764273	MK764339	MK764317	[53]
N. alpapicalis	MFLUCC 17–2544^T	MK357772	MK463545	MK463547	[54]
N. alpapicalis	MFLUCC 17–2545	MK357773	MK463546	MK463548	[54]
N. amomi	HKAS 124563^T	OP498012	OP752133	OP653489	[33]
N. amomi	HKAS 124564^T	OP498013	OP765913	OP753382	[33]
N. aotearoa	CBS 36754^T	NR163673	KM199454	KM199526	[1]
N. asiatica	MFLUCC12–0286^T	JX398983	JX399018	JX399049	[1]
N. australis	CBS 114159^T	KM199348	KM199432	KM199537	[1]
N. brachiata	MFLUCC 17–1555^T	MK764274	MK764340	MK764318	[53]
N. brasiliensis	COAD 2166^T	MG686469	MG692400	MG692402	[44]
N. camelliae–oleiferae	CSUFTCC81^T	OK493585	OK562360	OK507955	[55]
N. camelliae-oleiferae	CSUFTCC82	OK493586	OK562361	OK507956	[55]
N. cavernicola	KUMCC 20–0332	MW581238	MW59032	MW590327	[56]
N. cavernicola	KUMCC 20–0269^T	MW545802	MW557596	MW550735	[56]
N. chiangmaiensis	MFLUCC 19–0048	MW248391	MH412725	MW259070	[57]
N. chrysea	MFLUCC12–0261^T	JX398985	JX399020	JX399051	[1]
N. chrysea	MFLUCC12–0262	JX398986	JX399021	JX399052	[1]
N. clavispora	MFLUCC12–0281^T	JX398979	JX399014	JX399045	[1]
N. clavispora	MFLUCC12–0280	JX398978	JX399013	JX399044	[1]
N. cocoes	MFLUCC 15–0152^T	KX789687	–	KX789689	[58]
N. coffeae–arabicae	HGUP4015^T	KF412647	KF412641	KF412644	[59]
N. coffeae–arabicae	HGUP4109	KF412649	KF412643	KF412646	[59]
N. cubana	CBS 600 96^T	KM199347	KM199438	KM199521	[1]
N. cubana	CSUFTCC37	OK493583	OK562358	OK507953	[1]
N. cubana	CSUFTCC42	OK493584	OK562359	OK507954	[1]
N. cubana	GMBUCC 24–001	PP800244	PP889282	–	This study
N. dendrobii	MFLUCC 14–0106^T	MK993571	MK975835	MK975829	[60]
N. drenthii	BRIP 72264a	MZ303787	MZ312680	MZ344172	[22]
N. egyptiaca	PEST1/CBS 140162^T	KP943747	KP943746	KP943748	[61]
N. elaeidis	MFLUCC 15–0735^T	ON650689	–	ON734012	[62]
N. ellipsospora	MFLUCC12–0283^T	JX398980	JX399016	JX399047	[1]
N. eucalypticola	CBS 264 37^T	KM199376	KM199431	KM199551	[1]
N. eucalyptorum	CBS 147684^T	MW794108	MW802841	MW805397	[63]
N. foedans	CGMCC 3 9123^T	JX398987	JX399022	JX399053	[1]
N. foedans	CGMCC 3 9178	JX398989	JX399024	JX399055	[1]
N. formicarum	CBS 362 72^T	KM199358	KM199455	KM199517	[1]
N. formicarum	CBS 115 83	KM199344	KM199444	KM199519	[1]
N. fragariae	ZHKUCC 22–0115	ON651145	ON685199	ON685197	[64]
N. guajavae	FMB0026^T	MF783085	MH460871	MH460868	[65]
N. guajavicola	MFLUCC 22–0134^T	OP802393	OP801770	OP830892	[65]
N. hadrolaeliae	VIC 47180^T	MK454709	MK465120	MK465122	[66]
N. haikouensis	SAUCC212271^T	OK087294	OK104870	OK104877	[67]
N. haikouensis	SAUCC212272	OK087295	OK104871	OK104878	[67]
N. hispanica	FMB–Guv–B3^T	MW794107	MW802840	MW805399	[63]
N. honoluluana	CBS 114495^T	KM199364	KM199457	KM199548	[1]
N. honoluluana	CBS 111535	KM199363	KM199461	KM199546	[1]
N. hydeana	MFLUCC 20–0132^T	MW266069	MW251119	MW251129	[68]
N. hyperici	KUNCC 22–12597^T	OP498010	OP765908	OP713768	[33]
N. hyperici	KUNCC 22–12598	OP498009	OP737883	OP737880	[33]
N. Iberica	XF6	OM333900	OM350157	OM171265	[63]
N. Iberica	CBS 147688^T	MW794111	MW802844	MW805402	[63]
N. iranensis	P815^T	KM074048	KM074057	KM074051	[69]
N. iranensis	P814	KM074045	KM074056	KM074053	[69]
N. javaensis	CBS 257 31^T	NR_145241	KM199437	KM199543	[1]
N. longiappendiculata	MEAN–1315^T	MW794112	MW802845	MW805404	[63]
N. lusitanica	MEAN 1320	MW794097	MW802830	MW805409	[63]
N. lusitanica	MEAN–1317	MW794110	MW802843	MW805406	[63]
N. macadamiae	BRIP 63737c^T	KX186604	KX186654	KX186629	[25]
N. macadamiae	BRIP 63742a	KX186599	KX186657	KX186627	[25]
N. maddoxii	BRIP 72266a^T	MZ303782	MZ312675	MZ344167	[22]
N. magna	MFLUCC 12–0652^T	KF582795	KF582793	KF582791	[1]
N. mesopotamica	CBS 33686^T	KM199362	KM199441	KM199555	[1]

(to be continued)

Table 1. (continued)

Species	Culture collection number	ITS	*tub2*	*tef1*	Ref.
N. mianyangensis	CGMCC 323554^{T}	OP546681	OP672161	OP204793	[70]
N. mianyangensis	UESTCC 22–0006	OP082291	OP235979	OP204793	[70]
N. musae	MFLUCC 22–0162	OP802388	OP801765	OP830887	[58]
N. musae	MFLUCC 15–0776^{T}	KX789683	KX789686	KX789685	[58]
N. natalensis	CBS 138.41^{T}	NR_156288	KM199466	KM199552	[1]
N. nebuloides	BRIP 66617^{T}	OM417249	ON995130	ON624181	[71]
N. nebuloides	BRIP 70567	OM417295	ON995131	ON624201	[71]
N. olumideae	BRIP 72273a^{T}	MZ303790	–	–	[22]
N. olumideae	BRIP 72283a	MZ303791	MZ312684	MZ344176	[22]
N. paeoniae–suffruticosae	KUMCC 21–0426^{T}	OP082292	OP235980	OP204794	[70]
N. paeoniae–suffruticosae	KUMCC 21–0427	ON426868	OR025933	OR025972	[70]
N. pandanicola	MFLUCC 22–0144	OP802391	OP801768	OP830890	[57]
N. pernambucana	RV01^{T}	KJ792466	–	KU306739	[72]
N. perukae	FMB 0127	MH209077	MH460876	MH523647	[65]
N. petila	MFLUCC 17–1738^{T}	MK764276	MK764341	MK764319	[53]
N. petila	MFLUCC 17–1737	MK764275	MK764342	MK764320	[53]
N. phangngaensis	MFLUCC 18–0119^{T}	MH388354	MH412721	MH388390	[57]
N. photiniae	GUCC 21–0820	OP806524	OP896200	OP828691	[33]
N. photiniae	GUCC 810^{T}	OP498008	OP752131	OP753368	[33]
N. piceana	CBS 254 32	KM199372	KM199452	KM199529	[1]
N. piceana	CBS 394 48^{T}	KM199368	KM199453	KM199527	[1]
N. protearum	CBS 114178^{T}	JN712498	KM199463	KM199542	[1]
N. psidii	FMB 0028^{T}	MF783082	MH477870	MH460874	[65]
N. rhapidis	GUCC21501	MW931620	MW980441	MW980442	[34]
N. rhizophorae	MFLUCC 17–1551^{T}	MK764277	MK764343	MK764321	[53]
N. rhododendri	GUCC 21504^{T}	MW979577	MW980443	MW980444	[34]
N. rhododendricola	KUN–HKAS–123204^{T}	OK283069	OK274147	OK274148	[73]
N. rosae	CBS 101057^{T}	KM199359	KM199429	KM199523	[1]
N. rosicola	CFCC 51992^{T}	KY885239	KY885245	KY885243	[74]
N. rosicola	CFCC 51993	KY885240	KY885246	KY885244	[74]
N. samarangensis	CBS 115451	KM199365	KM199447	KM199556	[1]
N. saprophytica	MFLUCC12–0282^{T}	JX398982	JX399017	JX399048	[1]
N. scalabiensis	NJZSN01	OP942341	–	–	[43]
N. scalabiensis	GMBUCC 24–002	PP800245	PP889283	PP889285	This study
N. scalabiensis	GMBUCC 24–003	PP800246	PP889284	PP889286	This study
N. sichuanensis	SM15–1C	MW166232	MW218525	MW199751	[74]
N. siciliana	AC49	ON117811	ON209164	ON107275	[75]
N. siciliana	CBS 149117^{T}	ON117813	ON209162	ON107273	[75]
N. sonneratiae	MFLUCC 17–1744	MK764279	MK764345	MN871990	[53]
N. sonneratiae	MFLUCC 17–1745^{T}	MK764280	MK764346	MK764324	[53]
N. steyaertii	IMI 192475^{T}	KF582796	KF582794	KF582792	[1]
N. suphanburiensis	NGL–2022c isolate TN01^{T}	OP497994	OP752135	OP753372	[33]
N. surinamensis	CBS 450 74 T	KM199351	KM199465	KM199518	[1]
N. terricola	YMD A254/CGMCC 3 23553^{T}	OP082294	OP235983	OP204797	[70]
N. terricola	UESTCC 22.0034	OP082295	OP235983	OP204797	[70]
N. thailandica	MFLUCC 17–1730^{T}	MK764281	MK764347	MK764325	[53]
N. thailandica	MFLUCC 17–1731	MK764282	MK764348	MK764326	[53]
N. umbrinospora	MFLUCC12–0285^{T}	JX398984	JX399019	JX399050	[1]
N. vaccinii	1–22^{T}	OQ316613	–	OQ342778	[43]
N. vacciniicola	CAA1055^{T}	MW969751	MW934614	MW959103	[43]
N. vheenae	BRIP 72293a^{T}	MZ303792	MZ312685	MZ344177	[22]
N. vitis	JZB340018^{T}	KU140694	KU140685	KU140676	[76]
N. vitis	JZB340023	KU140699	KU140690	KU140681	[76]
N. xishuangbannaensis	KUMCC 21–0424^{T}	ON426865	OR025934	OR025973	[77]
N. xishuangbannaensis	KUMCC 21–0425	ON426866	OR025935	OR025974	[77]
N. zakeelii	BRIP 72282a^{T}	MZ303789	MZ312682	MZ344174	[22]
Pestalotiopsis trachycarpicola	OP068/IFRDCC 2240^{T}	JQ845947	JQ845945	JQ845946	[78]

Ex-type strains are indicated in ^{T}. The strains generated in this study are denoted in red.

et al.[52]) against pestalotioid species was tested. The cultures were obtained from the culture collection of the Genetics and Molecular Biology Unit, University of Sri Jayewardenapura (GBMUCC), and the Culture Collection of the University of Kelaniya (UKBC), Sri Lanka. PDA plates were divided into two portions. Fungal plugs of 4 mm diameter from the isolated fungal phytopathogens (GMBUCC 24–001, GMBUCC 24–002, and GMBUCC 24–003) and the bio–control agents were placed side by side in the two separated

portions, known as test plates (Fig. 1). They were triplicated for each pathogen. Plates containing pathogenic fungi without bio–control agents were used as control plates. Both control and test plates were incubated for 10 d at room temperature (25 ± 2 °C). The percentage of inhibition of fungal growth was calculated using the following formula proposed by Imtiaj & Lee[41]:

$$I\% = \frac{r_1 - r_2}{r_1} \times 100$$

where, r_1 is the radial growth of the isolated *Neopestalotiopsis* species in the control plates (cm), and r_2 is the radial growth of the *Neopestalotiopsis* species in the test plates (cm).

Results

Phylogeny

The combined data set of ITS, *tub2*, and *tef1* sequences comprised 1500 characters with gaps. The RAxML analysis of the combined dataset yielded a best-scoring tree (Fig. 2) with a final ML optimization likelihood value of –8738.944811. The matrix had 736 distinct alignment patterns, with 15.36 % of undetermined characters or gaps. Estimated base frequencies: A = 0.231055, C = 0.266487, G = 0.215875, T = 0.286583; substitution rates AC = 1.042093, AG = 3.330012, AT = 1.383087, CG = 0.619927, CT = 4.040718, GT = 1.000000; proportion of invariable sites I = 0.395452; gamma distribution shape parameter α = 0.657974. The Bayesian analysis resulted in 10,000 trees after 1,000,000 generations. All analyses (ML and BYPP) gave similar results and were in agreement with previous study based on multigene analyses[33].

Taxonomy

Neopestalotiopsis cubana Maharachchikumbura SSN, K.D. Hyde & Crous, Studies in Mycology 79: 138 (2014) [MB#809765] Fig. 3.

Associated with leaf lesions of *G. mangostana*, black spots emerge from the plant epidermis. **Sexual morph**: Undetermined. **Asexual morph**: Conidiomata pycnidial in culture on PDA, globose, solitary or aggregated, embedded or semi–immersed, dark brown to black, exuding globose, brown to black conidial masses. *Conidiophores* are reduced to conidiogenous cells. *Conidiogenous cells* 5–12 × 2–8 µm ($\bar{x}$ = 8.6 × 5.1, n = 25), discrete, cylindrical to subcylindrical, or ampulliform to lageniform, hyaline, smooth–walled. *Conidia* fusoid, ellipsoid, straight to slightly curved, somewhat constricted at septa, 4–septate, 19–27 × 7.5–10 µm ($\bar{x}$ = 23.4 × 8.7, n = 25); basal cell obconic to conic with a truncate base, hyaline, rogose and thin–walled, 3–5 µm long; three median cells doliform 14.5–16.5 µm long ($\bar{x}$= 15.6, n = 25), wall rugose, versicolored, septa darker than the rest of the cell; apical cell 4–5 µm long, hyaline, subcylindrical, thin– and smooth–walled; with 2–4 tubular apical appendages (mostly 3), arising from the apical + unbranched, filiform, flexuous, 21–28 µm long ($\bar{x}$= 24.6, n = 25), basal appendage single, tubular, unbranched, centric, 4–7 µm long.

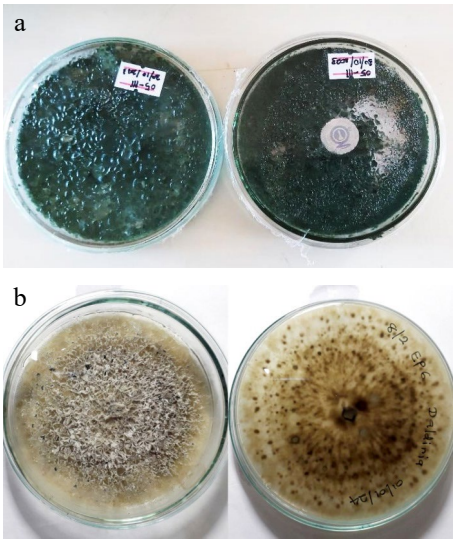

Fig. 1 Pure cultures of bio–control agents used in this study. (a) *Trichoderma atroviride* (GMBUCC 24–014) isolated from the basidiocarp of *Ganoderma angustisporum*. (b) *Daldinia eschscholtzii* (UKBC 036) isolated from the leaves of *Camellia sinensis* as an endophyte.

Culture characteristics: Colonies on PDA reaching 30–40 mm diameter after 7 d at room temperature (28 °C), with a lobate edge, pale honey–colored, with sparse aerial mycelium on the surface with black, gregarious conidiomata; reverse similar in color.

Known distribution: Cuba[1], Sri Lanka (this study).

Material examined: Sri Lanka, Western province, Gampaha District, Kadawatha, associated with fresh leaves of *Garcinia mangostana* (Mangosteen); 22 August 2022; Collector – K.M. Thambugala; USJ–GMBU–007; Culture – GMBUCC 24–001.

Notes: In the present phylogeny, the new isolate *N. cubana* (GMBUCC 24–001) clustered with *N. cubana* (CBS 600.96) from Cuba[23], suggesting that they are closely related (Fig. 2, Clade A). Clade A contains *N. cubana* CBS 600.96 (ex-type), LHHN37, LHHN42, GMBUCC 24–001 and *N. pandanicola* (MFLUCC 22–0144). When compared morphologically, our collection of *N. cubana* (GMBUCC 24–001) exhibits a slightly smaller conidial size and basal appendage length than *N. cubana* (CBS 600.96). Specifically, the conidial size of *N. cubana* (CBS 600 96) measures 22–31 × 7.5–9.0 µm, whereas *N. cubana* (GMBUCC 24–001) measures 19–27 × 5.5–8.5 µm. The basal appendage length of *N. cubana* (CBS 600.96) is 22–66 µm, whereas 20–50 µm for *N. cubana* (GMBUCC 24–001). Additionally, our collection has the same number of apical appendages, around 2–4 compared to *N. cubana* (CBS 600 96)[1]. In other conidial morphologies and colony characteristics, both strains exhibit similar patterns.

When compared to *N. cubana* (CBS 600.96), *N. pandanicola* (MFLUCC 22–0144) exhibits significantly different sizes of conidia and apical appendages. Specifically, the conidial size of *N. cubana* (CBS 600.96) measures 22–31 × 7.5–9.0 µm, whereas *N. pandanicola* (MFLUCC 22–0144) measures 16–25 × 4–7 µm. The apical appendage length of *N. cubana* (CBS 600 96) is 22–66 µm, while it is 27–30 µm for *N. pandanicola* (MFLUCC 22–0144). Additionally, basal appendage length is 6–11 µm long for *N. cubana* (CBS 600 96), and 3–7 µm for *N. pandanicola* (MFLUCC 22–0144). In addition to that, *N. pandanicola* (MFLUCC 22–0144) has a slight difference in apical appendages with 2–3 compared to 1–2 in *N. cubana* (CBS 600.96)[1,12,42]. In other conidial morphologies and colony characteristics, both strains exhibit similar patterns.

Neopestalotiopsis scalabiensis J. Santos, S. Hilário & A. Alves, Eur. J. Pl. Pathol. 162: 547 (2021) [MB#841333] Fig. 4.

Associated with small leaf lesions of *Annona muricata*, appear as black spots emerging from the plant epidermis surface. **Sexual morph**: Undetermined. **Asexual morph**: Conidiomata on PDA pycnidial, globose, solitary, semi–immersed, black, exuding globose, dark conidial masses; Conidiophores rare 15–27 × 3–4 µm ($\bar{x}$ = 21.3 × 3.7, n = 25); Conidiogenous cells discrete, cylindrical, hyaline, smooth–walled, tapering towards a truncate apex, 1.4–2 × 2.5–3 µm ($\bar{x}$ = 11.5 × 2.8, n = 25); Conidia fusoid, ellipsoid, straight to slightly curved, 3–4 septate, three median cells, wall rugose, versicolored, dark septa 13–15 × 5–7 µm ($\bar{x}$ = 14.5 × 6.2, n = 25); basal cell conic with a truncate base, hyaline, rugose 3–6 × 2–4 µm ($\bar{x}$ = 4.8 × 2.9, n = 25), with a short appendage 2.0–10 µm long; apical cell, hyaline, cylindrical, smooth–walled, 2.5–5 × 2–3.5 µm long ($\bar{x}$ = 3.7 × 2.6,

n = 25), with 2–3 tubular apical appendages, each inserted in the upper half of the apical cell, unbranched, filiform, 6.5–30 μm long ($\bar{x}$ = 19.3, n = 25).

Culture characteristics: Pycnidia developing on fennel twigs and pine needles, 70–90 mm diameter, after one week at room temperature on PDA. Colonies spreading on PDA with cottony flattened mycelium growing in a radial pattern with white cottony tufts resembling waves foam. Developing rare solitary black conidiomata with age and reverse white to snow white.

Known distribution: Portugal[43], Sri Lanka (this study)

Material examined: Sri Lanka, Western Province, Gampaha District, Kadawatha, associated with leaves of *Annona muricata* (Soursop); 22 August 2023; Collector – K.M. Thambugala; USJ–GMBU–008, and USJ–GMBU–009; Cultures– GMBUCC 24–002 and GMBUCC 24–003.

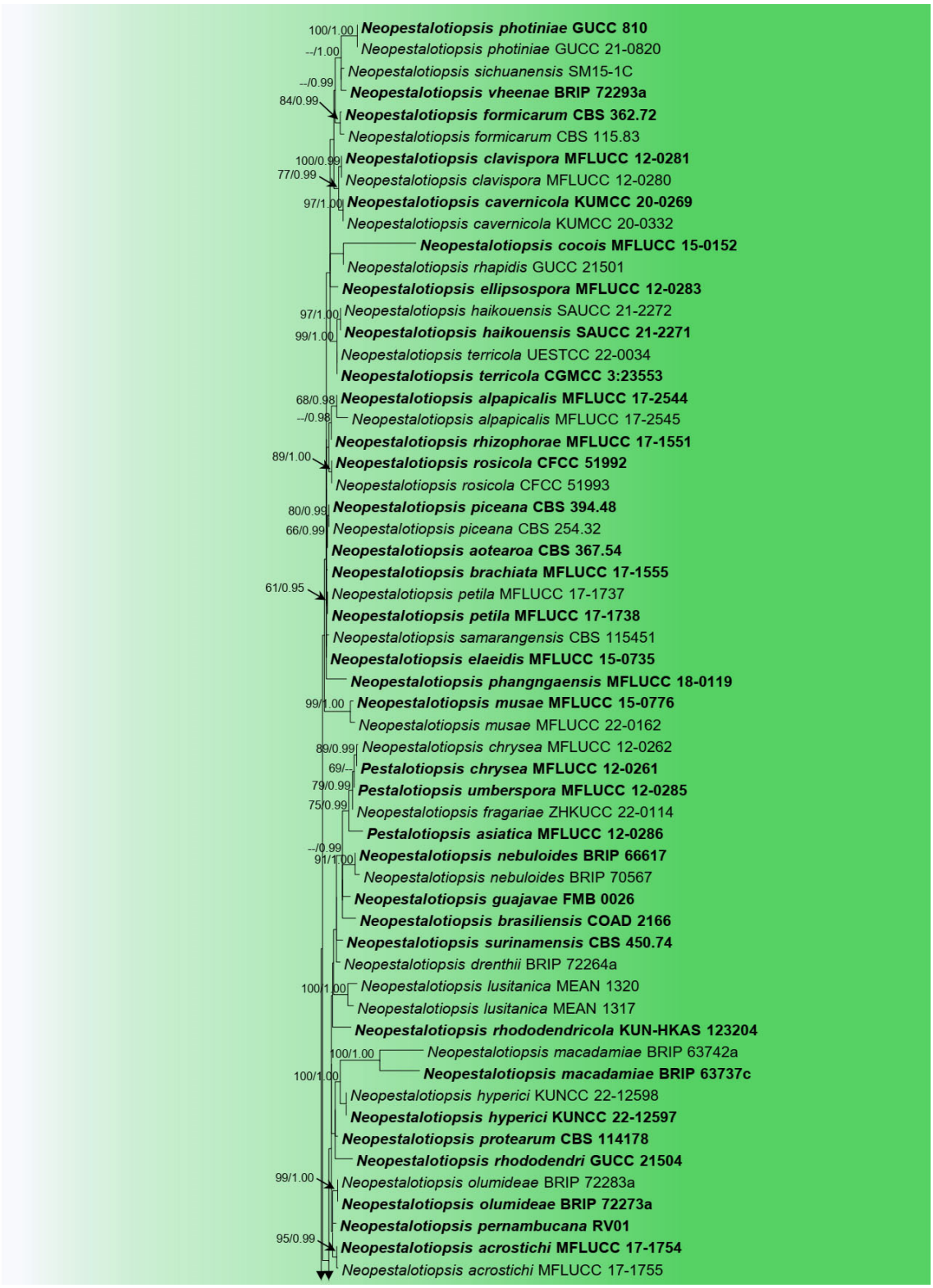

Fig. 2 (to be continued)

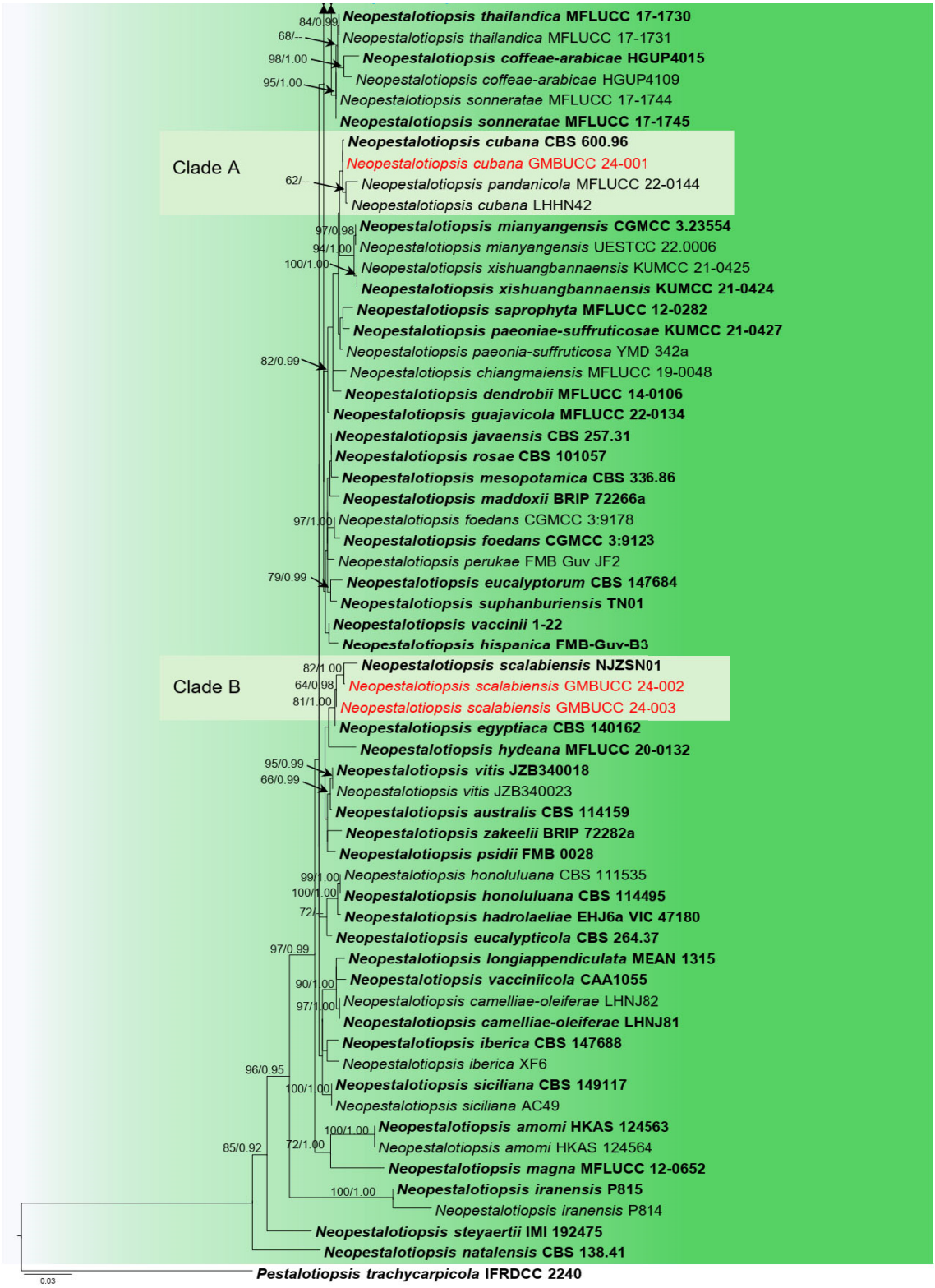

Fig. 2 Phylogram obtained based on ITS, *tub2*, and *tef1* sequencing data. The tree is rooted with *Pestalotiopsis trachycarpicola* (OP068). The bootstrap support values for maximum likelihood (≥ 50%) and Bayesian posterior probabilities (≥ 0.95) are shown at the nodes. The type strains are indicated in bold. Newly generated strains are in red.

Notes: In this study, the strain, GMBUCC 24–002, isolated from *A. muricata* in Sri Lanka, clustered together with *N. scalbiensis* (NJZSN01)[29] from *Vaccinium corymbosum* in Portugal, indicating that they are closely related (ML/MP/PP = 82/1.00) (Fig. 2, Clade B). The strain, GMBUCC 24–003, isolated from *A. muricata*, clustered together with *N. egyptiaca* (CBS 140162)[44], indicating that they are closely related (ML/MP/PP = 81/1.00) (Fig. 2, Clade B). The current collections of *N. scalabiensis* (GMBUCC 24–002 and GMBUCC 24–003) exhibit shorter basal appendages, measuring 2–10 μm, compared to *N. scalabiensis* (NJZSN01), which has appendages

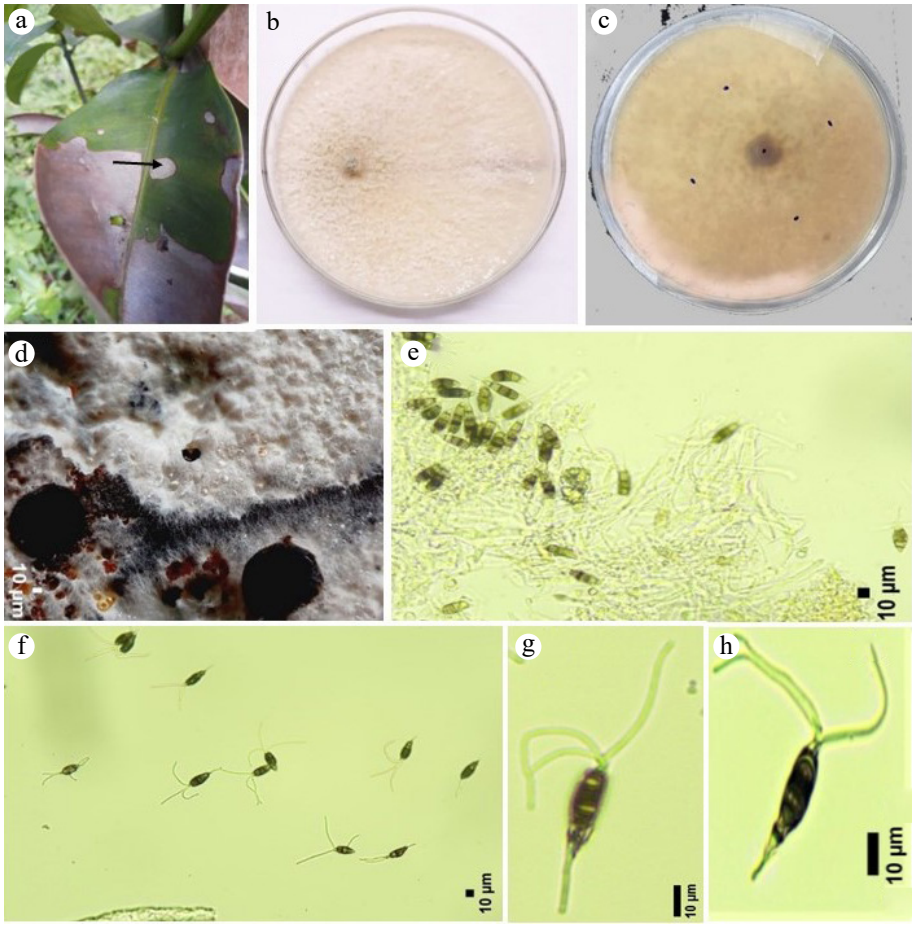

Fig. 3 *Neopestalotiopsis cubana* – (GMBUCC 24–001). (a) Leaf lesions on the host. (b), (c) Mycelial growth on PDA above and reverse. (d) Colony sporulating on PDA. (e) Conidiogenesis. (f)–(h) Conidia with appendages.

ranging from 2.1–17 µm. This difference in basal appendage length may be attributed to their distinct geographical origins. Furthermore, these collections of *N. scalabiensis* (GMBUCC 24–002 and GMBUCC 24–003) exhibit longer basal appendages, measuring 2–10 µm, compared to *N. egyptiaca* (CBS 140162), which has appendages ranging from 1.5–5.5 µm and longer apical appendages measuring 6.5–30 µm compared to *N. egyptiaca* (CBS140162), which has appendages ranging from 11-21 µm. Despite these variations, both strains exhibit similar conidial morphologies and colony characteristics, indicating a close relationship between the Sri Lankan collections (GMBUCC 24–002 and GMBUCC 24–003), the collections from Portugal (*N. scalabiensis* – NJZSN01) and Egypt (*N. egyptiaca* – CBS140162).

Dual culture assay

Trichoderma atroviride (GMBUCC 24–014) as the biocontrol agent (Tables 2 & 3).

Daldinia eschscholtzii (UKBC 036) as the biocontrol agent (Tables 4 & 5).

Discussion

Phytopathogenic fungi have been the primary focus of mycological research in Sri Lanka to date[26,45,46]. This emphasis arises from the significant impact of these fungal pathogens on plants and the resulting economic losses. Numerous investigations have been conducted to clarify the variety of pestalotioid species associated with various plants in Sri Lanka[1,47,79]. This study revealed the first record of *Neopestalotiopsis* species associated with *G. mangostana* and *A. muricata* in Sri Lanka. Fruits of *Manilkara zapota* infected by *Pestalotiopsis microspora* were first identified in Sri Lanka[48]. Recently, Weerasekara et al.[79] revealed multiple species of *Pseudopestalotiopsis* associated with grey blight in tea crops [*Camellia sinensis* (L.) O. Kuntze] in Sri Lanka. Among them, the currently known species of *Ps. daweiana, Ps. annellata,* and *Ps. chinensis* were identified based on the molecular data derived from ex-type isolates. Additionally, four new species of *Pseudopestalotiopsis* viz *Ps. petchii, Ps. ratnapurensis, Ps. rossmaniae,* and *Ps. srilankensis* were introduced. Nevertheless, it is evident that economically significant plants such as *G. mangostana* and *A. muricata* are also affected by pestalotioid pathogens.

In this study, three gene regions—ITS, *tub2*, and *tef1*-α were used for PCR amplification. These universal primers were selected to offer substantial infra– and interspecific variation that makes them effective for species identification and phylogenetic analysis[49]. While this study focused on these three gene regions, future research could benefit from incorporating large subunit rRNA (LSU) and RNA polymerase II second-largest subunit (RPB2) to enhance phylogenetic resolution.

The results revealed the presence of *Neopestalotiopsis* species—*N. cubana* (GMBUCC 24–001) associated with *G. mangostana* leaves and *N. scalabiensis* (GMBUCC 24–002 and GMBUCC 24–003) associated with *A. muricata* leaves. Phylogenetic analysis indicates that these *Neopestalotiopsis* species from *G. mangostana* and *A. muricata* do not form closely related groups, as they are placed in different clades (Fig. 2, Clades A and B). This divergence may be attributed to host specificity. Notably, *N. cubana* (GMBUCC 24–001) clusters as a

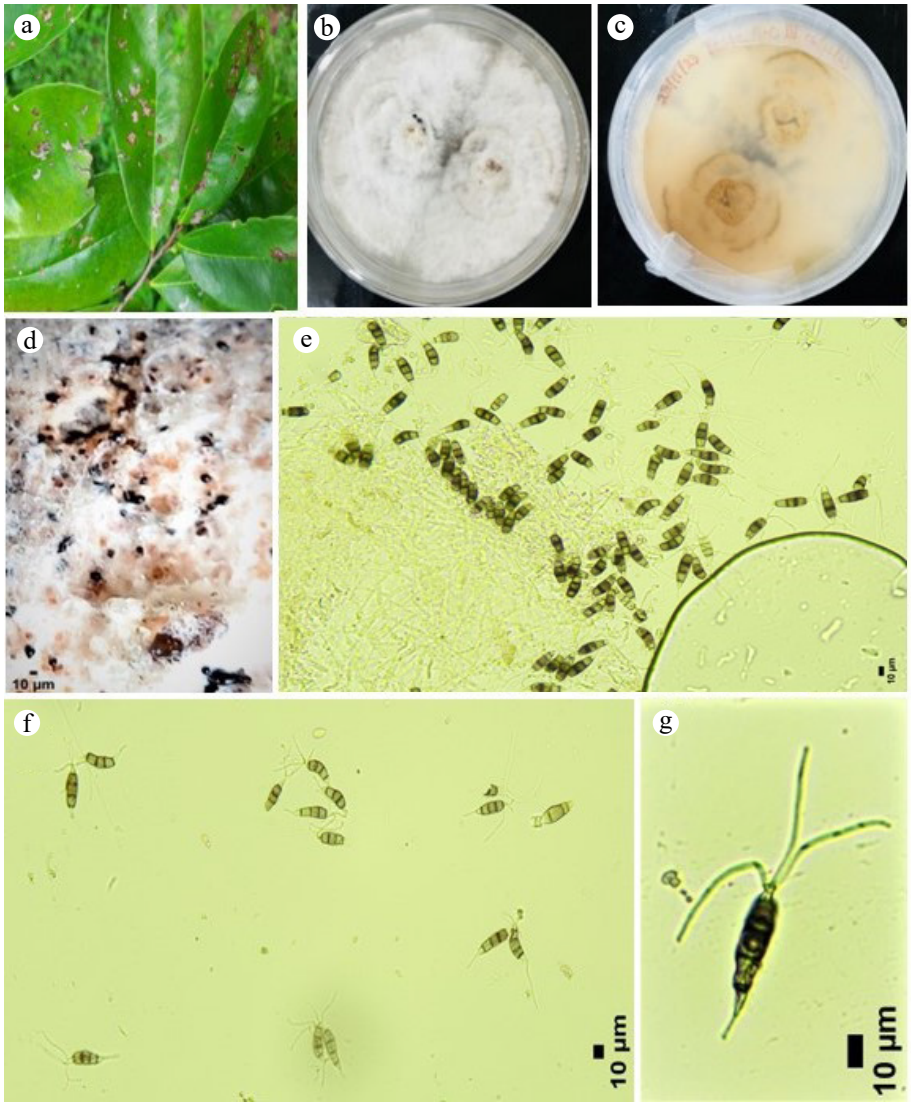

Fig. 4 *Neopestalotiopsis scalabiensis* – (GMBUCC 24–002 and GMBUCC 24–003). (a) Leaf lesions on the host. (b), (c) Mycelial growth on PDA above and reverse. (d) Colony sporulating on PDA (conidiomata). (e) Conidiogenesis. (f), (g) Conidia with appendages.

Table 2. *In vitro* biocontrol estimation of *T. atroviride* (GMBUCC 24–014) against *N. cubana* (GMBUCC 24–001) associated with the leaves of *G. mangostana*.

Day	Control (r_1/cm)	T1 (r_2/cm)	T2 (r_2/cm)	T3 (r_2/cm)	Average (r_2\cm)	I%
3	0.5	0.3	0.5	0.3	0.37	26.0
5	1.5	1.1	1	1.2	1.1	26.7
7	1.7	1.1	1	1.2	1.1	35.3
10	2	1.2	1	1.2	1.1	45.0

Table 3. *In vitro* biocontrol estimation of *T. atroviride* (GMBUCC 24–014) against *N. scalabiensis* (GMBUCC 24–002, and GMBUCC 24–003) associated with the leaves of *A. muricata*.

Date	Control (r_1/cm)	T1 (r_2/cm)	T2 (r_2/cm)	T3 (r_2/cm)	Average (r_2/cm)	I%
3	1.5	0.5	1	1.3	0.93	38.0
5	2	0.5	1.5	1.5	1.16	42.0
7	2.5	0.7	1.5	1.5	1.23	50.8
10	3	0.7	1.5	1.5	1.23	59.0

r_1: growth radian of the pathogen (*Neopestalotiopsis* species) without biocontrol agent (*T. atroviride*), r_2: growth radian of the pathogen (*Neopestalotiopsis* species) in the presence of biocontrol agent (*T. atroviride*), C: control, T1/T2/T3: test replicates, I: inhibition percentage.

sister taxon to *N. cubana* (CBS 600 96) from Cuba[1], suggesting a close relationship (Fig. 2, Clade A). Despite there being some variations, both isolated strains of *N. scalabiensis* (GMBUCC 24–002 and GMBUCC 24–003) exhibit similar conidial morphologies and colony characteristics, indicating a close relationship with the collections from Portugal (*N. scalabiensis* – NJZSN01) and Egypt (*N. egyptiaca* – CBS140162) (Fig. 2, Clade B). Further clarification of this species' phylogenetic position would require a detailed examination of morphological characteristics and the inclusion of additional molecular markers.

It is important to note that we did not include pathogenicity testing in this study to confirm the disease-causing potential of the *Neopestalotiopsis* species isolated from *A. muricata* and *G. mangostana*. While Koch's postulates were not fulfilled in the study, the isolates were included in an *in vitro* evaluation based on the well-documented pathogenic potential of several *Neopestalotiopsis* species across diverse host plants. However, we recognize that pathogenicity tests are essential to establish a definitive causal relationship between fungal isolates and host symptoms. As such, our findings should be considered preliminary and not conclusive regarding the role of isolates as pathogens. Future work will focus

Table 4. *In vitro* biocontrol estimation of *D. eschscholtzii* (UKBC 036) against *N. cubana* (GMBUCC 24–001) associated with the leaves of *G. mangostana*.

Day	Control (r_1/cm)	T1 (r_2/cm)	T2 (r_2/cm)	T3 (r_2/cm)	Average (r_2\cm)	I%
3	0.5	0.3	0.6	0.5	0.46	8.0
5	1.5	1.1	1.3	1	1.13	24.6
7	1.7	1.1	1.5	1.2	1.26	25.8
10	2	1.2	1.5	1.2	1.3	35.0

Table 5. *In vitro* biocontrol estimation of *D. eschscholtzii* (UKBC 036) against *N. scalabiensis* (GMBUCC 24–002, and GMBUCC 24–003) associated with the leaves of *A. muricata*.

Date	Control (r1/cm)	T1 (r2/cm)	T2 (r2/cm)	T3 (r2/cm)	Average (r2/cm)	I%
3	1.5	1	1.3	1	1.1	26.0
5	2	1.2	1.6	1.5	1.36	32.0
7	2.3	1.5	2.0	1.5	1.3	33.6
10	2.5	1.5	2.0	1.5	1.3	46.7

r1: growth radian of the pathogen (pestalotioid species) without biocontrol agent (*Daldinia eschscholtzii*), r2: growth radian of the pathogen (pestalotioid species) in the presence of biocontrol agent (*Daldinia eschscholtzii*), C: control, T1/T2/T3: test replicates, I: inhibition percentage.

on conducting pathogenicity assays and in planta biocontrol trials to validate the *in vitro* observations and evaluate the practical application of these fungal biocontrol agents in disease management.

Fungal biocontrol agents not only prevent diseases but also promote plant growth, enhance nutrient utilization efficiency, strengthen plant resistance, and mitigate agrochemical pollution in the environment[50]. In the dual culture assay, both *T. atroviride* (GMBUCC 24–014) and *Daldinia eschscholtzii* (UKBC 036) showed significant percentages of inhibition against *N. scalabiensis* (GMBUCC 24–002 and GMBUCC 24–003) which is around 59% and 47% respectively (Fig. 5). In addition to that, *T. atroviride* (GMBUCC 24–014) shows higher biocontrol potential over *D. eschscholtzii* (UKBC 036) on *N. cubana* (GMBUCC 24–001), and *N. scalabiensis* (GMBUCC 24–002 and GMBUCC 24–003). This suggests that *T. atroviride* (GMBUCC 24–014) can be a potential biocontrol agent against *N. cubana* (GMBUCC 24–001), and *N. scalabiensis* (GMBUCC 24–002 and GMBUCC 24–003) compared to *D. eschscholtzii* (UKBC 036).

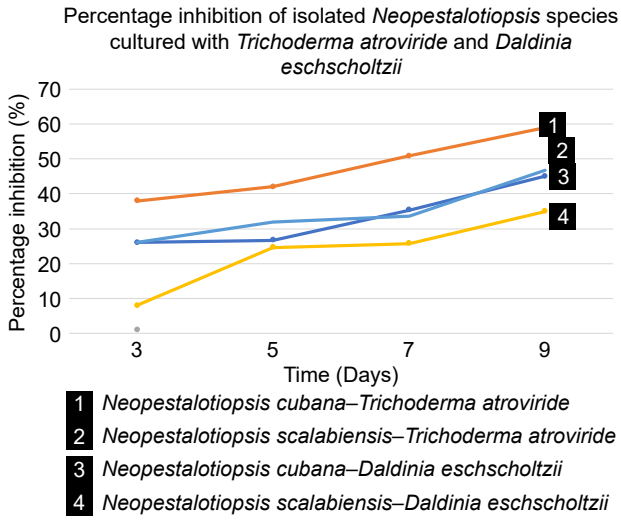

Fig. 5 *In vitro* biocontrol estimation of *T. atroviride* (GMBUCC 24–014) and *Daldinia eschscholtzii* (UKBC 036) against the isolated species (*N. cubana* – GMBUCC 24–001; *N. scalabiensis* – GMBUCC 24–002, and GMBUCC 24–003).

The structural complexity and biological activity of the secondary metabolites produced by pestalotioid species have drawn attention to them. Several new secondary metabolites have been isolated and discovered in recent decades[7]. Their bioactivities, which include anticancer, antifungal, antibacterial, and nematocidal activity, as well as medical, agricultural, and industrial applications, were investigated[1,2,7]. It would be beneficial to identify the symbiont pathogens with pestalotioid species since their bioactive metabolites can also have inhibitory action against pestalotioid species.

Conclusions

This study has significantly advanced the understanding of the fungi associated with leaf lesions of *G. mangostana* and *A. muricata* plants from Sri Lanka, identifying two *Neopestalotiopsis* species. For the first time, *N. cubana* (GMBUCC 24–001) from *G. mangostana*, and *N. scalabiensis* (GMBUCC 24–002 and GMBUCC 24–003) from *A. muricata* reported. The presence of various Pestalotioid fungi indicates that the leaf lesions of *G. mangostana* and *A. muricata* are diverse, demanding further research to establish the fungal communities associated with the disease. These insights are crucial for developing better biocontrol agents and management practices in this plant cultivation. *T. atroviride* (GMBUCC 24–014) shows higher biocontrol potential over *Daldinia eschscholtzii* (UKBC 036); this suggests that *T. atroviride* (GMBUCC 24–014) can be a potential biocontrol agent against both isolated species compared to *Daldinia eschscholtzii* (UKBC 036).

Author contributions

The authors confirm contribution to the paper as follows: conceptualization, data curation, and formal analysis: Asfa F, Thambugala KM, de Silva NI; funding acquisition: Liyanage KK, Thambugala KM, Tennakoon S; investigation, methodology, and writing – original draft: Asfa F, Thambugala KM, Daranagama DA, Tennakoon S; supervision: Thambugala KM; writing, review, and editing: Asfa F, Thambugala KM, de Silva NI, Daranagama DA. All authors reviewed the results and approved the final version of the manuscript.

Data availability

The data generated and analyzed during this study are available in this article. DNA sequence data are available in the GenBank database, and the accession numbers are provided in Table 1. ITS: PP800244, PP800245, PP800246, PP859452; *tub*: PP889282, PP889283, PP889284; *tef1-α*: PP889285, PP889286.

Acknowledgments

The research was supported by the Center for Plant Materials and Herbal Products Research, University of Sri Jayewardenepura, Nugegoda 10250, Sri Lanka; Rubber Research Institute, Sri Lanka (RRISL), Dartonfield, Agalawatta, Sri Lanka; Centre for Biotechnology (CBT), Department of Zoology, Center for Forestry and Environment, Department of Forestry and Environment Sciences, Faculty of Applied Sciences, University of Sri Jayewardenepura; and the Department of Plant and Molecular Biology, Faculty of Science, University of Kelaniya, Kelaniya 11300, Sri Lanka.

Conflict of interest

The authors declare that they have no conflict of interest.

Dates

Received 26 February 2025; Revised 6 May 2025; Accepted 6 May 2025; Published online 18 June 2025

References

1. Maharachchikumbura SSN, Hyde KD, Groenewald JZ, Xu J, Crous PW. 2014. *Pestalotiopsis* revisited. *Studies in Mycology* 79:121–86
2. Wu C, Wang Y, Yang Y. 2022. *Pestalotiopsis* diversity: species, dispositions, secondary metabolites, and bioactivities. *Molecules* 27(22):8088
3. Zhang W, Li Y, Lin L, Jia A, Fan X. 2024. Updating the Species Diversity of Pestalotioid Fungi: Four New Species of *Neopestalotiopsis* and *Pestalotiopsis*. *Journal of Fungi* 10(7):475
4. Jeewon R, Liew ECY, Hyde KD. 2002. Phylogenetic relationships of *Pestalotiopsis* and allied genera inferred from ribosomal DNA sequences and morphological characters. *Molecular Phylogenetics and Evolution* 25(3):378–92
5. Jeewon R, Liew ECY, Simpson JA, John Hodgkiss I, Hyde KD. 2003. Phylogenetic significance of morphological characters in the taxonomy of *Pestalotiopsis* species. *Molecular Phylogenetics and Evolution* 27(3):372–83
6. Nozawa S, Yamaguchi K, Hoang Yen LT, Van Hop D, Phay N, et al. 2017. Identification of two new species and a sexual morph from the genus *Pseudopestalotiopsis*. *Mycoscience* 58(5):328–37
7. Maharachchikumbura SSN, Guo LD, Chukeatirote E, Bahkali AH, Hyde KD. 2011. *Pestalotiopsis*—morphology, phylogeny, biochemistry and diversity. *Fungal Diversity* 50(1):167–87
8. Corda ACJ. 1842. *Icones fungorum hucusque cognitorum*. Prague, Czech: JG Calve. pp. 1–92.
9. Hyde KD, Noorabadi MT, Thiyagaraja V, He MQ, Johnston PR, et al. 2024. The 2024 Outline of Fungi and fungus-like taxa. *Mycosphere* 15(1):5146–6239
10. Liu AR, Chen SC, Wu SY, Xu T, Guo LD, et al. 2010. Cultural studies coupled with DNA based sequence analyses and its implication on pigmentation as a phylogenetic marker in Pestalotiopsis taxonomy. *Molecular Phylogenetics and Evolution* 57(2):528–35
11. Ariyawansa H. Hyde KD. 2018. Additions to *Pestalotiopsis* in Taiwan. *Mycosphere* 9(5):999–1013
12. Lee Y, Kim GH, Kim Y, Park SY, Koh YJ. 2019. First report of twig dieback caused by *Neopestalotiopsis clavispora* on blueberry in Korea. *Plant Disease* 103(5):1022
13. Rodríguez-Gálvez, E, Hilário, S, Lopes, A. Alves, A. 2020. Diversity and pathogenicity of *Lasiodiplodia* and *Neopestalotiopsis* species associated with stem blight and dieback of blueberry plants in Peru. *European Journal of Plant Pathology* 157(1):89–102
14. Guterres DC, Silva MA, Martins MD, Azevedo DMQ, Lisboa DO, et al. 2023. Leaf spot caused by *Neopestalotiopsis* species on Arecaceae in Brazil. *Australasian Plant Pathology* 52(1):47–62
15. Gerardo-Lugo SS, Tovar-Pedraza JM, Maharachchikumbura SSN, Apodaca-Sánchez MA, Correia KC, et al. 2020. Characterization of *Neopestalotiopsis* species associated with mango grey leaf spot disease in Sinaloa, Mexico. *Pathogens* 9(10):788
16. Shi J, Li B, Wang S, Zhang W, Shang M, et al. 2024. Occurrence of *Neopestalotiopsis clavispora* causing Apple leaf spot in China. *Agronomy* 29;14(8):1658
17. Rebollar-Alviter A, Silva-Rojas HV, Fuentes-Aragón D, Acosta-González U, Martínez-Ruiz M, et al. 2020. An emerging strawberry fungal disease associated with root rot, crown rot and leaf spot caused by *Neopestalotiopsis rosae* in Mexico. *Plant Disease* 16;104(8):2054–59
18. Biju CN, Peeran MF, Gowri R. 2018. Identification and characterization of *Neopestalotiopsis clavispora* associated with leaf blight of small cardamom (*Elettaria cardamomum* Maton). *Journal of Phytopathology* 166(7–8):532–46
19. Shahriar SA, Nur-Shakirah AO, Mohd MH. 2022. *Neopestalotiopsis clavispora* and *Pseudopestalotiopsis camelliae-sinensis* causing grey blight disease of tea (*Camellia sinensis*) in Malaysia. *European Journal of Plant Pathology* 62:709–24
20. Darapanit A, Boonyuen N, Leesutthiphonchai W, Nuankaew S, Piasai O. 2021. Identification, pathogenicity and effects of plant extracts on *Neopestalotiopsis* and *Pseudopestalotiopsis* causing fruit diseases. *Scientific Reports* 11:22606
21. Baggio JS, Forcelini BB, Wang NY, Ruschel RG, Mertely JC, et al. 2021. Outbreak of leaf spot and fruit rot in Florida strawberry caused by *Neopestalotiopsis* spp. *Plant Disease* 105(2):305–15
22. Prasannath K, Shivas RG, Galea VJ, Akinsanmi OA. 2021. *Neopestalotiopsis* species associated with flower diseases of *Macadamia integrifolia* in Australia. *Journal of Fungi* 7(9):771
23. Akinsanmi OA, Nisa S, Jeff-Ego OS, Shivas RG, Drenth A. 2017. Dry flower disease of *Macadamia* in Australia Caused by *Neopestalotiopsis macadamiae* sp. nov. and *Pestalotiopsis macadamiae* sp. nov. *Plant Disease* 101(1):45–53
24. Pornsuriya C, Chairin T, Thaochan N, Sunpapao A. 2020. Identification and characterization of *Neopestalotiopsis* fungi associated with a novel leaf fall disease of rubber trees (*Hevea brasiliensis)* in Thailand. *Journal of Phytopathology* 168(7–8):416–27
25. Thaochan N, Pornsuriya C, Chairin T, Sunpapao A. 2020. Roles of systemic fungicide in antifungal activity and induced defense responses in rubber tree (*Hevea brasiliensis*) against leaf fall disease caused by *Neopestalotiopsis cubana*. *Physiological and Molecular Plant Pathology* 111:101511
26. Okubo-Kurihara E, Febbiyanti TR, Ashari F, Yanagawa Y, Osada E, et al. 2024. Screening of effective pesticides to control rubber tree leaf fall disease (LFD) caused by *Neopestalotiopsis* and *Colletotrichum* fungi in Indonesia. *Journal of Pesticide Science* 20;49(4):277–84
27. Adikaram NKB, Maharachchikumbura SSN, Yakandawala DMD, Manawadu LN, Dissanayake DMS, et al. 2023. Postharvest stem-end browning (SEB) disease in ripe mango (*Mangifera indica* L.) cultivar TomEJC. *European Journal of Plant Pathology* 165(3):447–64
28. Ávila-Hernández JG, León-Ramírez CG, del Rosario Abraham-Juárez M, Tlapal-Bolaños B, Olalde-Portugal V, et al. 2025. *Neopestalotiopsis* spp.: a threat to strawberry production and management. *Horticulturae* 11(3):288
29. Thambugala KM, Hyde KD, Tanaka K, Tian Q, Wanasinghe DN, et al. 2015. Towards a natural classification and backbone tree for Lophiostomataceae, Floricolaceae, and Amorosiaceae fam. nov. *Fungal Diversity* 74(1):199–266
30. Glass NL, Donaldson GC. 1995. Development of primer sets designed for use with the PCR to amplify conserved genes from filamentous ascomycetes. *Applied and Environmental Microbiology* 61(4):1323–30
31. White T, Bruns T, Lee S, Taylor J. 1990. Amplification and direct sequencing of fungal ribosomal RNA genes for phylogenetics. *PCR protocols: A Guide to Methods and Applications* 18:315–22
32. Groenewald M, Lombard L, de Vries M, Lopez AG, Smith M, et al. 2018. Diversity of yeast species from Dutch garden soil and the description of six novel Ascomycetes. *FEMS Yeast Research* 18(7):foy076
33. Sun YR, Jayawardena RS, Sun JE, Wang Y. 2023. Pestalotioid species associated with medicinal plants in southwest China and Thailand. *Microbiology Spectrum* 11:e0398722
34. Yang Q, Zeng XY, Yuan J, Zhang Q, He YK, et al. 2021. Two new species of *Neopestalotiopsis* from southern China. *Biodiversity Data Journal* 9:e70446
35. Stamatakis A. 2014. RAxML version 8: a tool for phylogenetic analysis and post-analysis of large phylogenies. *Bioinformatics* 30(9):1312–13
36. Stamatakis A, Hoover P, Rougemont J. 2008. A Rapid Bootstrap Algorithm for the RAxML Web Servers. *Systematic Biology* 57(5):758–71
37. Huelsenbeck JP, Ronquist F. 2001. MRBAYES: Bayesian inference of phylogenetic trees. *Bioinformatics* 17(8):754–55
38. Rannala B, Yang Z. 1996. Probability distribution of molecular evolutionary trees: a new method of phylogenetic inference. *Journal of Molecular Evolution* 43(3):304–11
39. Zhaxybayeva O, Gogarten JP. 2002. Bootstrap, Bayesian probability and maximum likelihood mapping: exploring new tools for comparative genome analyses. *BMC Genomics* 3:4
40. Rambaut A. 2012. *FigTree version 1.4.0*. http://tree.bio.ed.ac.uk/software/figtree
41. Imtiaj A, Lee TS. 2008. Antagonistic effect of three *Trichoderma* species on the *Alternaria porri* pathogen of onion blotch. *World Journal of Agricultural Sciences* 4(1):13–17

42. Seifollahi E, de Farias ARG, Jayawardena RS, Hyde KD. 2023. Taxonomic advances from fungal flora associated with ferns and fern-like hosts in northern Thailand. *Plants* 12(3):683
43. Santos J, Hilário S, Pinto G, Alves A. 2022. Diversity and pathogenicity of pestalotioid fungi associated with blueberry plants in Portugal, with description of three novel species of *Neopestalotiopsis*. *European Journal of Plant Pathology* 162(3):539–555
44. Bezerra JDP, Machado AR, Firmino AL, Rosado AWC, de Souza CAF, et al. 2018. Mycological diversity description I. *Acta Botanica Brasilica* 32(4):656–66
45. Anthony S, Abeywickrama K, Dayananda R, Wijeratnam S, Arambewela L. 2004. Fungal pathogens associated with banana fruit in Sri Lanka, and their treatment with essential oils. *Mycopathologia* 157(1):91–97
46. Ekanayake G, Abeywickrama K, Daranagama A, Kannangara S. 2019. Morphological characterization and molecular identification of stem-end rot associated fungal species isolated from "Karutha Colomban" mango fruits in Sri Lanka. *Journal of Agricultural Sciences – Sri Lanka* 14(2):120
47. Pandey AK, Sinniah GD, Yadav S, Maharachchikumbura SSN. 2023. *Pestalotiopsis*-like species: host network and lifestyle on tea crop. *Fungal Biology Reviews* 47:100340
48. Wijayawardene NN, Hyde KD, Al-Ani LKT, Tedersoo L, Haelewaters D, et al. 2020. Outline of fungi and fungus-like taxa. *Mycosphere* 11(1):1060–456
49. Stielow JB, Lévesque CA, Seifert KA, Meyer W, Iriny L, et al. 2015. One fungus, which genes? Development and assessment of universal primers for potential secondary fungal DNA barcodes. *Persoonia - Molecular Phylogeny and Evolution of Fungi* 35(1):242–63
50. Thambugala KM, Daranagama DA, Phillips AJL, Kannangara SD, Promputtha I, et al. 2020. Fungi vs. fungi in biocontrol: an overview of fungal antagonists applied against fungal plant pathogens. *Frontiers in Cellular and Infection Microbiology* 10:604923
51. Konara UA, Thambugala KM, Karunarathna SC, Ediriweera A, Hapuarachchi KK. 2024. Unveiling the hidden diversity of *Ganoderma* (Ganodermataceae, Polyporales) in Sri Lanka: the first report of *G. angustisporum*, *G. ellipsoideum*, and *G. orbiforme*. *New Zealand Journal of Botany* 18:1–25
52. Thambugala K, Daranagama D, Kannangara S, Kodituwakku T. 2021. Revealing the endophytic mycoflora in tea (*Camellia sinensis*) leaves in Sri Lanka: the first comprehensive study. *Phytotaxa* 514(3):247–60
53. Norphanphoun C, Jayawardena RS, Chen Y, Wen TC, Meepol W, et al. 2019. Morphological and phylogenetic characterization of novel pestalotioid species associated with mangroves in Thailand. *Mycosphere* 10(1):531–578
54. Kumar V, Cheewangkoon R, Gentekaki E, Maharachchikumbura SSN, Brahmanage RS, et al. 2019. *Neopestalotiopsis alpapicalis* sp. nov. a new endophyte from tropical mangrove trees in Krabi Province (Thailand). *Phytotaxa* 393(3):251–251
55. Li L, Yang Q, Li H. 2021. Morphology, phylogeny, and pathogenicity of pestalotioid species on *Camellia oleifera* in China. *Journal of Fungi,* 7(12):1080
56. Liu X, Tibpromma S, Zhang F, Xu J, Chethana KWT, et al. 2021. *Neopestalotiopsis cavernicola* sp. nov. from Gem Cave in Yunnan Province, China. *Phytotaxa* 512(1):1–27
57. Tibpromma S, Hyde KD, McKenzie EHC, Bhat DJ, Phillips AJL, et al. 2018. Fungal diversity notes 840–928: micro-fungi associated with Pandanaceae. *Fungal Diversity* 93(1):1–160
58. Hyde KD, Hongsanan S, Jeewon R, Bhat DJ, McKenzie EHC, et al. 2016. Fungal diversity notes 367–490: taxonomic and phylogenetic contributions to fungal taxa. *Fungal Diversity* 80(1):1–270
59. Song Y, Geng K, Hyde KD, Zhao WS, Wei JG, et al. 2013. Two new species of *Pestalotiopsis* from Southern China. *Phytotaxa* 126:22
60. Ma XY, Maharachchikumbura SSN, Chen BW, Hyde KD, McKenzie EHC, et al. 2019. Endophytic pestalotiod taxa in *Dendrobium orchids*. *Phytotaxa* 419(3):268–86
61. Crous PW, Wingfield MJ, Le Roux JJ, Richardson DM, Strasberg D, et al. 2015. Fungal Planet description sheets: 371–399. *Persoonia* 35(1):264–327
62. Konta S, Tibpromma S, Karunarathna SC, Samarakoon MC, Steven LS, et al. 2023. Morphology and multigene phylogeny reveal ten novel taxa in Ascomycota from terrestrial palm substrates (Arecaceae) in Thailand. *Mycosphere* 14(1):107–52
63. Diogo E, Gonçalves CI, Silva AC, Valente C, Bragança H, et al. 2021. Five new species of *Neopestalotiopsis* associated with diseased *Eucalyptus* spp. in Portugal. *Mycological Progress* 20(11):1441–56
64. Prematunga CJ, You LQ, Gomdola D, Balasuriya A, Yang YH, et al. 2022. An addition to pestalotioid fungi in China: *Neopestalotiopsis fragariae* sp. nov. causing leaf spots on *Fragaria* × *ananassa*. *Asian Journal of Mycology* 5(2):220–38
65. Ul Haq I, Ijaz S, Khan NA. 2021. Genealogical concordance of phylogenetic species recognition-based delimitation of Neopestalotiopsis species associated with leaf spots and fruit canker disease affected guava plants. *Pakistan Journal of Agricultural Sciences* 58(04):1301–1313
66. Freitas EFS, Da Silva M, Barros MVP, Kasuya MCM. 2019. *Neopestalotiopsis hadrolaeliae* sp. nov., a new endophytic species from the roots of the endangered orchid *Hadrolaelia jongheana* in Brazil. *Phytotaxa* 416(3):211–20
67. Zhang Z, Liu R, Liu S, Mu T, Zhang X, et al. 2022. Morphological and phylogenetic analyses reveal two new species of Sporocadaceae from Hainan, China. *MycoKeys* 88:171–92
68. Huanaluek N, Jayawardena RS, Maharachchikumbura SSN, Harishchandra DL. 2021. Additions to pestalotioid fungi in Thailand: *Neopestalotiopsis hydeana* sp. nov. and *Pestalotiopsis hydei* sp. nov. *Phytotaxa* 479(1):23–43
69. Ayoubi N, Soleimani MJ. 2016. Strawberry fruit rot caused by *Neopestalotiopsis iranensis* sp. nov. , and *N. mesopotamica*. *Current Microbiology* 72:329–36
70. Li WL, Dissanayake AJ, Zhang T, Maharachchikumbura SSN, Liu JK. 2022. Identification and pathogenicity of pestalotiod fungi associated with woody oil plants in Sichuan Province, China. *Journal of Fungi* 8(11):1175
71. Crous PW, Wingfield MJ, Chooi YH, Gilchrist CLM, Lacey E, et al. 2020. Fungal Planet description sheets: 1042–1111. *Persoonia - Molecular Phylogeny and Evolution of Fungi* 44(1):301–459
72. Lins Silvério M, de Queiroz Calvacanti MA, Alves da Silva G, Vilela de Oliveira RJ, Bezerra JL. 2016. A new epifoliar species of *Neopestalotiopsis* from Brazil. *Agrotrópica* 28(2):151–58
73. Chaiwan N, Jeewon R, Pem D, Jayawardena RS, Nazurally N, et al. 2022. Fungal Species from *Rhododendron* sp.: *Discosia rhododendricola* sp. nov, *Neopestalotiopsis rhododendricola* sp. nov and *Diaporthe nobilis* as a new host record. *Journal of Fungi* 8(9):907
74. Jiang N, Bonthond G, Fan X, Tian C. 2018. *Neopestalotiopsis* rosicola *sp. nov. causing stem canker of* Rosa chinensis *in China*. *Mycotaxon* 133(2):271–83
75. Fiorenza A, Gusella G, Aiello D, Polizzi G, Voglmayr H. 2022. *Neopestalotiopsis siciliana* sp. nov. and *N. rosae* Causing Stem Lesion and Dieback on Avocado Plants in Italy. *Journal of Fungi* 8(6):562–562
76. Jayawardena RS, Liu M, Maharachchikumbura SSN, Zhang W, Xing Q, et al. 2016. *Neopestalotiopsis vitis* sp. nov. causing grapevine leaf spot in China. *Phytotaxa* 258(1):63–74
77. Liu XF, Tibpromma S, Hughes AC, Chethana K, Wijayawardene NN, et al. 2023. Culturable mycota on bats in central and southern Yunnan Province, China. *Mycosphere* 14(1):497–662
78. Zhang Y, Maharachchikumbura SSN, McKenzie EHC, Hyde KD. 2012. A novel species of pestalotiopsis causing leaf spots of *Trachycarpus Fortunei*. *Cryptogamie, Mycologie* 33(3):311–18
79. Weerasekara IT, Udayanga D, Manamgoda DS, Mapa MST, Sinniah GD, et al. 2024. Morphological and molecular reassessment of *Pseudopestalotiopsis* in the gray blight complex of tea with four new species from Sri Lanka. *Mycological Progress* 23:72